DOI: 10.1002/stco.201800025

Markus Kuhnhenne, Dominik Pyschny*, Lisa Kramer, Matthias Brieden, Thomas Ummenhofer, Daniel C. Ruff, Christian Fauth, Rainer Holz

Mechanical and thermal performance of new liner tray solutions

Liner tray wall systems are widely used for industrial and commercial buildings. Up until now, the main type used was the conventional solution with a thin (3 mm) separation strip between liner tray and outer shell. In the meantime, various solutions exist on the market to improve the thermal performance of this wall system. On the one hand, this paper deals with numerical studies that show how these new solutions reduce the heat transfer coefficient of liner tray wall systems. On the other hand, it is about the related increase in the fixing distance s_1 and its influence on the mechanical performance of liner tray wall systems. Extensive experimental investigations have been performed on liner trays with a directly attached outer façade within the scope of the European RFCS Research Project GRISPE. Practicable calculation methods have been derived based on existing regulations and methods. This paper depicts by way of excerpts the results for liner trays with a directly attached outer façade for fastener distances that are not or insufficiently covered in the standards.

Keywords: lightweight metal construction; thin-walled cold-formed sections; liner trays; loadbearing capacity; thermal insulation; energy efficiency; effective insulation thickness

1 Introduction

In industrial and commercial buildings, liner trays are widely used as the inner layer of double-skin wall systems with thermal insulation combined with an outer façade layer. The multi-layered construction consists of a liner tray with a material thickness of 0.75–1.50 mm, an insulating material core whose thickness corresponds to the web depth of the liner tray, and profiled sheets (e.g. corrugated or trapezoidal profile or a rainscreen façade panel). The liner trays usually span horizontally from column to column. The loadbearing capacity of liner trays depend very much on the stabilization of the narrow top flange by the outer shell.

In the conventional construction of a liner tray wall system, the webs of the liner tray create a linear thermal bridge that has a decisive influence on the heat transfer coefficient and therefore on the heat exchange of the entire building envelope. This has led to the development of new liner tray systems that attempt to reduce this thermal bridge effect.

The most cost-efficient, and therefore most frequently used, solution is the one with a thermal separating strip. This strip consists of a material with a low thermal conductivity and is normally 3 mm thick, since according to EN 1090-4 [1], Annex B.6, intermediate layers up to a maximum thickness of 3 mm can be used without the need for a structural analysis. In order to reduce the heat transfer from the outer shell to the liner tray, the separating strip is attached to the narrow top flange of the liner tray, see Fig. 1, Option 1.

One option for improving the thermal performance of this conventional solution is to replace the thermal separation strip by additional insulation layers (40 or 80 mm of mineral wool, see Fig. 1, Option 2). Special self-drilling screws were developed for fastening the outer shell; they bridge the distance between the outer shell and the narrow flange. In this application the weight of the outer shell must either be suspended from the eaves or supported at the base.

Another way to improve the energy efficiency of liner tray wall systems is to use an additional insulation layer with the aid of spacer sections spanning vertically. Here, the outer shell can be formed with any façade profiles spanning horizontally. The spacer sections are attached to the narrow flanges of the liner tray and serve as a substructure for the façade layer (see Fig. 1, Option 3). In this option it is possible to fill the gap created by the spacer sections with thermal insulation in order to improve the thermal performance of the liner tray wall system. The influence of the different options for improving the thermal performance of liner tray wall systems is examined in more detail in the following section.

Compared with applications with directly attached external façade profiles, the shear stiffness of the external shell is significantly lower in systems with spacer sections. This leads to a lower stabilizing effect on the narrow flange of the liner tray. In addition, the distance between the spacer sections is often greater than that between the attachment points of the conventional application with a directly attached outer shell. The actual design rule for the fixing distance according to EN 1993-1-3 [2] is rather conservative and, furthermore, limited to a maximum fixing distance $s_1 = 1000$ mm. In order to determine and

*) Corresponding author: dpy@stb.rwth-aachen.de
Submitted for review: 09 October 2018
Accepted for publication: 06 December 2018

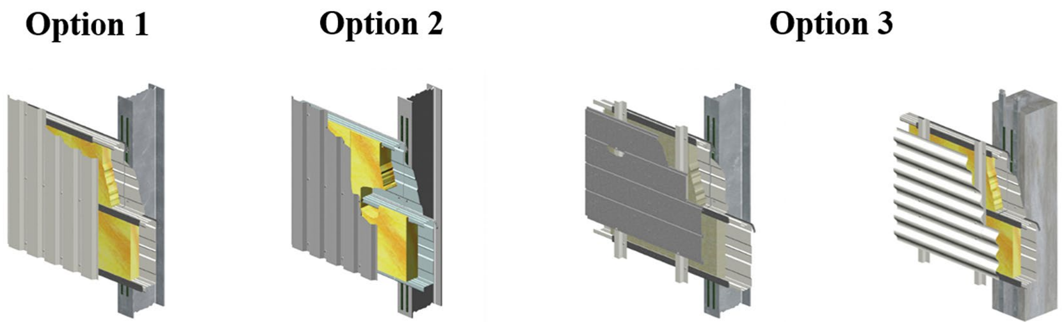

Fig. 1. Different options for liner tray wall systems

compare the loadbearing capacity of liner tray wall systems with larger fixing distances, an extensive testing programme was carried out at KIT Steel and Lightweight Structures and a practicable calculation method was derived within the scope of the European project GRISPE, see section 3.

2 Comparison of different options to improve the thermal performance of liner tray wall systems

2.1 General

The thermal performance of wall systems can be determined on the basis of EN ISO 6946 [3]. For homogeneous components, the standard contains manual calculation methods that can be used to determine the heat transfer coefficient. For inhomogeneous components without significant thermal bridge effects (especially without metallic thermal bridges), the thermal quality can also be calculated with the aid of EN ISO 6946.

Numerical methods based on EN ISO 10211 [4] should be used for components where multidimensional geometric or material-related thermal bridges have to be taken into account. This also includes the finite element method (FEM). Owing to the high thermal conductivity of steel, any steel components in the thermal insulation layer of the building envelope represent a material-related thermal bridge. For this reason, it is necessary to use numerical methods to assess the thermal quality of liner tray wall systems.

Fig. 1 shows different options for liner tray wall systems in order to improve their thermal performance and aesthetics. In option 1, a 3 mm separating strip between the warm liner tray (inside) and the cold trapezoidal profile (outside) is used to reduce the thermal bridge effect caused by the liner tray, but this is not enough to meet the current energy efficiency requirements of German energy-saving legislation. In option 2, the thermal bridging effect of the liner tray webs is reduced by including an additional thermal insulation layer between liner tray and trapezoidal profile fixed with special self-drilling screws. Option 3 uses spacer sections (Z or Ω sections) spanning vertically to serve as the substructure for the façade layer. Here, the gap created by the spacer sections could be filled with thermal insulation to improve the thermal performance.

Basically, improving the thermal performance of liner tray wall systems is also possible over cladding with sandwich panels. This option can be used, for example, during renovation work when the thermal insulation no longer meets current requirements, but for operational reasons it is not possible to dismantle the outer shell completely. Detailed information can be found in [5] and [6].

In order to show the efficiency of different options, numerical simulations have been carried out according to EN ISO 10211. The boundary conditions and results of these investigations are explained below.

2.2 Numerical simulations

To compare the heat transfer coefficients of the three options shown in Fig. 1, the following material parameters and dimensions were defined. A steel sheet thickness of 1.5 mm for the liner tray and a thermal conductivity of 0.035 W/(m·K) for the mineral wool were assumed for all options. The dimensions of the separating strip in option 1 are $d_{\mathrm{Sep}} = 3$ mm and $b_{\mathrm{Sep}} = 60$ mm. For option 2, two different cases were considered: $\Delta d_{\mathrm{c}} = 40$ mm and $\Delta d_{\mathrm{c}} = 80$ mm, see also Fig. 2.

Fig. 3 shows the two different spacer sections (Z and Ω sections) selected for option 3 and their dimensions. As the section depth is 60 mm, the thickness of the additional insulation material is also 60 mm. The maximum fixing distance $s_1 = 1000$ mm according to the calculation method of EN 1993-1-3 was selected for the fixing distance of the Z and Ω sections. Further information on the influence of this fixing distance on the loadbearing capacity of the overall structure can be found in section 3.

The thermal conductivities of the materials were defined according to DIN EN ISO 10456 [7], DIN 4108-4 [8] and IFBS-Fachinformation 4.02 [9]. Fig. 4 shows an FE model and the temperature distribution determined for option 3 with a Z section as an example. In the numerical simulations, a steel sheet without profiling was used as the external façade element. The reasons why this simplification is possible are explained in [10].

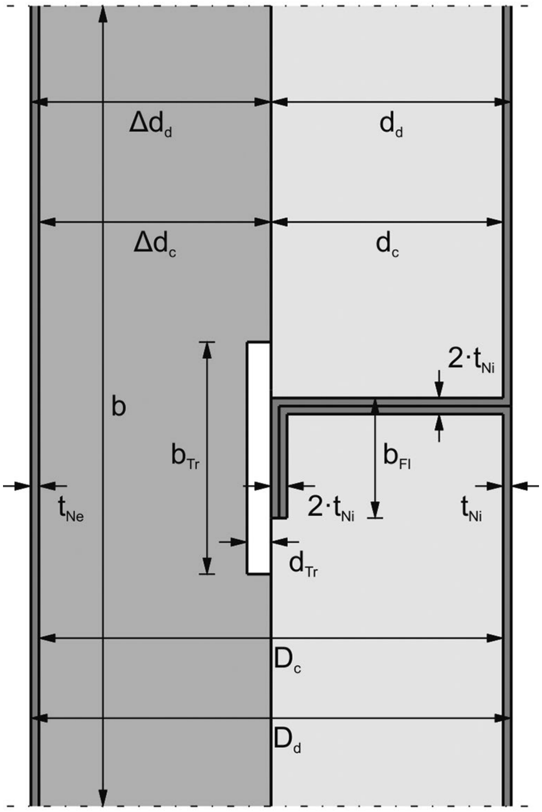

Fig. 2. Schematic section through liner tray construction

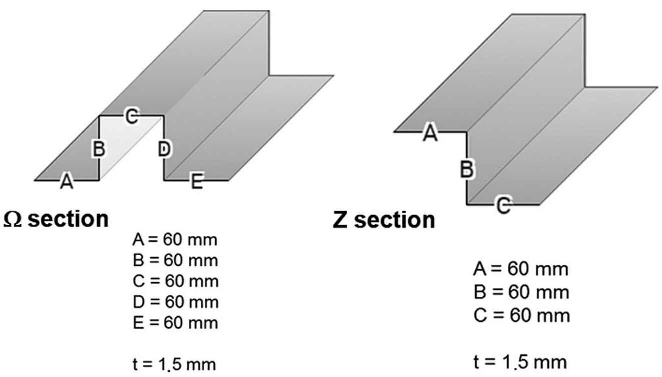

Fig. 3. Forms and dimensions of Ω and Z sections

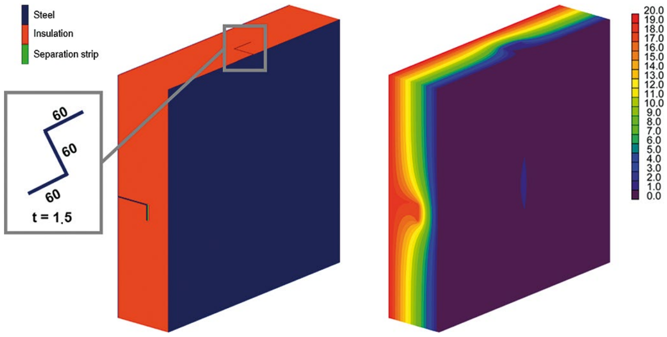

Fig. 4. Example of thermal FE model and temperature distribution of liner tray wall system for option 3 with Z section

2.3 Results

The results of the numerical investigations are summarized in Table 1. It can be seen that the liner tray wall system option 2 with an additional insulation layer is the best option for limiting the heat transfer between the outer shell and the liner tray. This design needs special self-drilling screws that bridge the distance between the outer shell and the narrow flange of the liner tray but are limited in their ability to carry transverse loads. In this application the weight of the outer shell must either be suspended from the eaves or supported at the base.

Option 3 shows that owing to the larger cross-sectional area of the Ω section ($A = 450$ mm^2) compared with the Z section ($A = 270$ mm^2), the thermal bridging effects created by the sections are different. The Ω section therefore generally leads to higher heat transfer coefficients.

Overall, the thermal performance of the conventional liner tray wall system (option 1) can be improved by the variants considered. The diagram in Fig. 5 shows the result of Table 1 by plotting the heat transfer coeffizients of the different options against the total insulation thickness.

The diagram in Fig. 6 shows that when using a 90 mm liner tray (t_N = 1.50 mm) based on a heat transfer co-

Table 1. Heat transfer coefficients of liner tray wall systems

	Heat transfer coefficient U [$W/(m^2 \cdot K)$]									
	Liner tray depth d_c [mm]									
	90	100	120	130	145	160	180	200	220	240
Option 1	0.844	0.806	0.744	0.718	0.684	0.654	0.620	0.590	0.563	0.540
Option 2 40 mm	0.338	0.324	0.303	0.294	0.283	0.273	0.262	0.253	0.245	0.238
Option 2 80 mm	0.239	0.232	0.219	0.214	0.207	0.201	0.195	0.189	0.184	0.180
Option 3 Ω section	0.381	0.371	0.351	0.341	0.326	0.318	0.308	0.298	0.287	0.277
Option 3 Z section	0.333	0.324	0.306	0.298	0.285	0.278	0.270	0.261	0.252	0.244

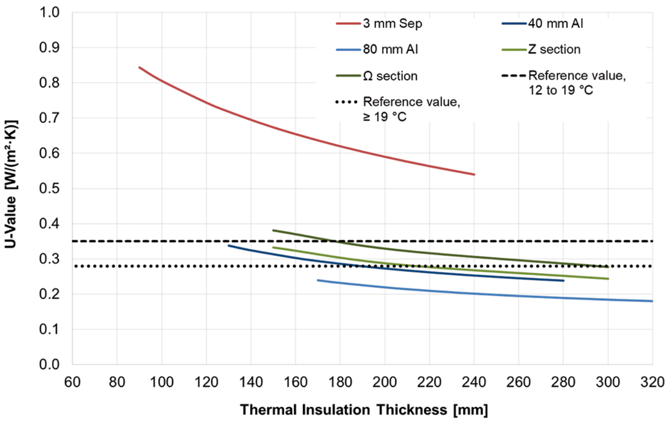

Fig. 5. Thermal performance of different liner tray wall systems

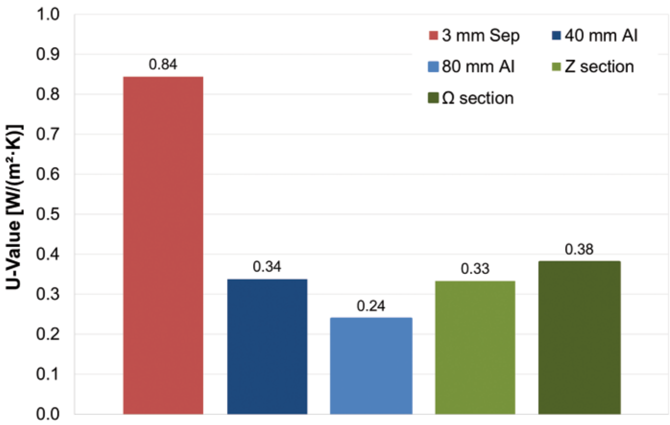

Fig. 6. Heat transfer coefficients of liner tray wall systems, example

efficient $U_d = 0.84\ W/(m^2 \cdot K)$ for option 1, a value $U_d = 0.34\ W/(m^2 \cdot K)$ can be achieved by (undisturbed) 40 mm additional insulation and $U_d = 0.24\ W/(m^2 \cdot K)$ by 80 mm additional insulation (option 2). If option 3 with a *Z* or *Ω* section is considered, a heat transfer coefficient $U_d = 0.33\ W/(m^2 \cdot K)$ or $U_d = 0.38\ W/(m^2 \cdot K)$ is the result.

3 Loadbearing behaviour of liner tray wall systems with fixing distances $s_1 > 1000$ mm

3.1 General

The loadbearing capacity of liner trays is usually determined by tests according to EN 1993-1-3 [1]. Here, reference is made in the National Annex [11] to DIN 18807-2 [12], DIN 18807-2/A1 [13] and the "Supplementary test principles for liner tray profiles". Tests are carried out to determine the shear resistance at an end support (end support test) and the mid-span moment resistance (single-span test) as well as the combination of moment and support reaction at the intermediate support (internal support test or double-span test), both for pressure and uplift loads. Since the loadbearing capacity is heavily dependent on the stabilization of the upper flanges, the tests are carried out with the corresponding outer cladding (trapezoidal profile, corrugated profile, etc.) and a defined fixing distance between outer cladding and liner tray profiles. Depending on the outer cladding, the fixing distance may vary between $s_1 = 210$ mm and $s_1 = 2000$ mm. At the fixing points of the infinitely shear-stiff outer cladding (with outer cladding directly adjacent or fixed via spacer sections), the upper flanges are stabilized against lateral buckling. The longer the distance between the fixings, the smaller is the supporting effect. Therefore, the load capacity values are only valid for fixing distances up to the tested distance s_1. The lateral support of the upper flanges is important if they are in compression. This applies especially to wind pressure in the span (positive bending moment caused by positive load) and wind suction at the intermediate support (positive bending moment caused by negative load).

If no corresponding test results are available, the loadbearing capacity may also be calculated according to EN 1993-1-3. When calculating the ultimate bending moment according to [1], section 10.2, it is necessary to distinguish between positive and negative bending moments. This distinction has to be made because of the supporting effect of the outer cladding on the upper flanges of the liner tray under positive bending moments and the different effective widths of the wide flange. Shear distortions can be neglected for standard liner trays. A detailed description of the step-by-step calculation can be found in [14].

In EN 1993-1-3, the influence of the lateral support of the upper flanges is taken into account by the coefficient β_b, which depends linearly on the fixing distance s_1.

$$\beta_b = 1.15 - s_1/2000 \quad (1)$$

This is based on the assumption that with a fixing distance $s_1 = 300$ mm, the upper flanges in compression are completely supported and thus lateral movement is prevented ($\beta_b = 1.0$). If the fixing distances s_1 are significantly longer than 300 mm, the method presented here leads to conservative design results. This is the case, for example, if the outer cladding attached horizontally (parallel to the direction of the liner trays) requires the use of spacer sections between the outer cladding and the liner trays. DIN 18807 does not specify a calculation method for the lateral support of the upper flanges under compressive stress.

3.2 Test results

To determine the influence of stabilization of the upper flanges through the almost shear-resistant outer cladding (trapezoidal profile in this case), liner trays were tested at KIT with different fixing distances s_1 within the scope of the RFCS project GRISPE. The stabilizing effect involves a positive bending moment in the span or a positive bending moment above the intermediate support. Therefore, single-span tests were carried out under pres-

Table 2. Test scope of liner trays for determining the loadbearing behaviour of different fixing distances s1

Specimen	Test	Nominal thickness t_N [mm]	L [mm]	Fixing distance s_1 [mm]
Liner trays: 110/600 and 160/600 trapezoidal profile: 35/207-0.75	Single-span test: pressure load	0.75 and 1.00	6000	621
				1242
				1863
				> 6000 (without fixings)
	Internal support test: uplift load	0.75 and 1.00	2000	621
				1242
				1863
				> 2000 (without fixings)

sure load and internal support tests under wind suction according to EN 1993-1-3, taking into account the national annex.

The single-span tests were carried out on two liner tray geometries in steel grade S320GD according to EN 10346 [15] with web depths of 110 and 160 mm and two nominal thicknesses of 0.75 and 1.00 mm. The width of the sections was 600 mm. A 35/207 trapezoidal profile in steel grade S320GD with a nominal thickness of 0.75 mm was used as a directly attached outer cladding. The test specimens consisted of one complete and two half liner trays. The trapezoidal profiles were fixed to the upper flanges of the liner trays with self-drilling screws at a distance s_1. The length of all liner tray specimens was 6400 mm and the overhang of each liner tray was 200 mm. The load was introduced into the trapezoidal outer sheet via transverse steel sections and timber blocks. Transverse ties prevented the profiles from spreading. At the end supports, timber blocks were used to avoid local deformation. The deflections were measured continuously at mid-span by three trip wire displacement sensors, the deflections were measured under the bottom flanges. The load was applied with displacement control at a rate of 20 mm/min and measured continuously using a load cell with a maximum capacity of 50 kN. The trapezoidal profiles as outer cladding were fixed to the upper flanges at a distance s_1. The scope of the tests and the relevant parameters are given in Table 2.

Owing to the compressive stress in the upper flanges, failure occurred due to local buckling of the upper flanges of the liner tray and the adjacent web as well as the edge stiffener (see Fig. 7). With longer distances between fasteners and deeper webs, lateral movement of the webs and upper flanges occurred instead of the local deformation (local buckling and distortional buckling). The test results were statistically evaluated according to EN 1993-1-3 and the characteristic span moment resistance was determined under gravity loading $M_{c,Rk,F}$.

Fig. 7. Local buckling of the upper flange of the liner tray between the outer cladding fixings – single-span positive bending test [16]

Fig. 8 plots the ratio between the characteristic span moment $M_{c,Rk,F,s1}$ for different fixing distances between the trapezoidal profile and the upper flanges (lateral support), relative to the reference value of the characteristic span moment resistance $M_{c,Rk,F,621mm}$ at s_1 = 621 mm, as a function of the fixing distance for the four types of liner tray examined. The reduction in the bending load capacity can be described as a function of the fixing distance and the slenderness of the webs and upper flanges. The longer the fixing distance and the higher the slenderness of the elements of the cross-section in compression, the lower is the bending moment resistance (Fig. 8).

The reduction in the bending moment resistance with a larger fixing distance s_1 can be explained by the fact that a larger fixing distance s_1 results in weaker lateral support for the upper flange and thus a smaller torsional restraint, which leads to a lower torsional flexural buckling capacity of the member. The ultimate stress of the upper flange and the adjoining web limits the bending moment resistance of the liner trays.

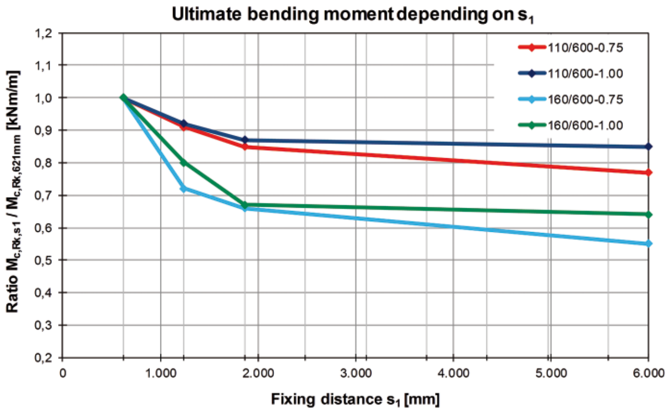

Fig. 8. Ratio between $M_{c,Rk,F,s1}$ and $M_{c,Rk,F,621mm}$ depending on fixing distance s_1

3.3 New design method for greater fixing distances s_1 with outer cladding directly attached

In the course of GRISPE, a calculation method was derived based on EN 1993-1-3. The aim of the method was to convert known load capacity values at a defined distance of the lateral support $s_{1,1}$ (fixing distance of upper flange) to deviating fixing distances $s_{1,2}$. In this method the compressive forces $N_{Rk,i,s1,1}$ that can be absorbed by the flanges of the liner tray are calculated for the reference distance of the lateral support $s_{1,1}$ of the elastic bedded beam in compression (upper flange and web), taking into account local buckling of the plane cross-section parts and distortional buckling of the edge stiffener. The elastic bedding is taken into account by the stiffness of the liner tray in the transverse direction. The fixing distance $s_{1,1}$ is represented by the bearing of the elastically bedded beam in compression perpendicular to the web of the liner tray. Owing to the different geometry, both narrow flanges must be calculated separately. The characteristic compression load $N_{Rk,i,s1,2}$ is then calculated for the required distance $s_{1,2}$. The load capacity of the upper flanges with identical fixing distance $s_{1,i}$ is added and set in relation. This ratio describes the reduction in the compressive force that can be absorbed by the upper flanges in relation to the reference value. The ultimate bending moment of the total liner tray cross-section is reduced to the same extent as the ultimate flange compressive force (e.g. characteristic value of bending moment resistance at distance $s_{1,1}$ in this case). So the ultimate bending moment at distance $s_{1.2}$ is

$$M_{c,Rk,2} = M_{c,Rk,1} \cdot \beta = M_{c,Rk,1} \cdot \frac{\sum N_{Rk,i,s_{1,2}}}{\sum N_{Rk,i,s_{1,1}}} \tag{2}$$

Thus, the characteristic values of the span moment under pressure load or the supporting moment under uplift load for a distance $s_{1,2}$ can be calculated from values already known for a given distance $s_{1,1}$ (e.g. from a type approval certificate or DOP). The steps of the procedure are described in detail below. Owing to the different geometries, steps 1 to 3 must be applied separately for both upper flanges.

Step 1: Calculation of the gross cross-section of the compressed flanges (upper flange, edge stiffener and 1/5 of web) according to EN 1993-1-3.

Step 2: Calculation of the effective cross-section of the compressed flanges considering local buckling (effective widths of plane elements) and distortional buckling (effective thickness of edge stiffener) according to EN 1993-1-3. The calculation is for a compressive stress $\sigma_{com,Ed}$ (initially selected, improved by iteration).

Step 3: Calculation of the compressive force of the cross-section considering the lateral evasion on an elastically bedded beam with a fixing distance s_1. The fixing brackets and the bedding are positioned transverse to the clamping direction of the liner trays. The elastic bedding of the small web is used assuming a symmetrical deformation of the wide flange as follows:

$$K_{fz} = \frac{E \cdot t^3}{12 \cdot \left(1 - \nu^2\right)} \cdot \frac{6}{2 \cdot h^3 + 3 \cdot b \cdot h^2} \tag{3}$$

The critical axial force N_{cr} for an elastically bedded beam with discrete fasteners at a distance s_1 is

$$N_{cr} = \frac{n^2 \cdot \pi^2 \cdot E \cdot I_{fz}}{s_1^2} + \frac{K_{fz} \cdot s_1^2}{n^2 \cdot \pi^2} \tag{4}$$

As a rule, the minimum results for $n = 1$ (a half-wave between the fastenings), but for larger fixing distances, the second eigenmode with $n = 2$ (two half-waves between the fastenings) must also be examined. The calculation of the ultimate compressive force that can be absorbed is similar to EN 1993-1-3, where buckling curves a_0 and c are examined as an alternative. With the reduction coefficient χ determined in this way, the actual stress σ_{Ed} is now calculated. If the stress σ_{Ed} differs from the compressive stress $\sigma_{com,Ed}$ selected in step 2, steps 2 and 3 are repeated with the stress $\sigma_{com,Ed} = \sigma_{Ed}$ until the compressive stress selected in step 2 and the calculated stress σ_{Ed} from step 3 are equal (iterative procedure).

Step 4: Determination of the reduction coefficient by addition of the ultimate compressive forces for both effective cross-sections at identical fixing distances $s_{1,i}$. The reduction coefficient β for distance $s_{1,2}$ is

$$\beta = \frac{N_{Rk,1,s_{1,2}} + N_{Rk,2,s_{1,2}}}{N_{Rk,1,s_{1,1}} + N_{Rk,2,s_{1,1}}} \tag{5}$$

The characteristic ultimate bending moment for fixing distance $s_{1,2}$ is then calculated as follows:

$$M_{c,Rk,2} = M_{c,Rk,1} \cdot \beta \tag{6}$$

Fig. 9 shows the results of this calculation method, the calculated reductions according to EN 1993-1-3, section 10.2.2.2, and the test results, each related to the reference value (s_1 = 621 mm). When using buckling curve a_0 in

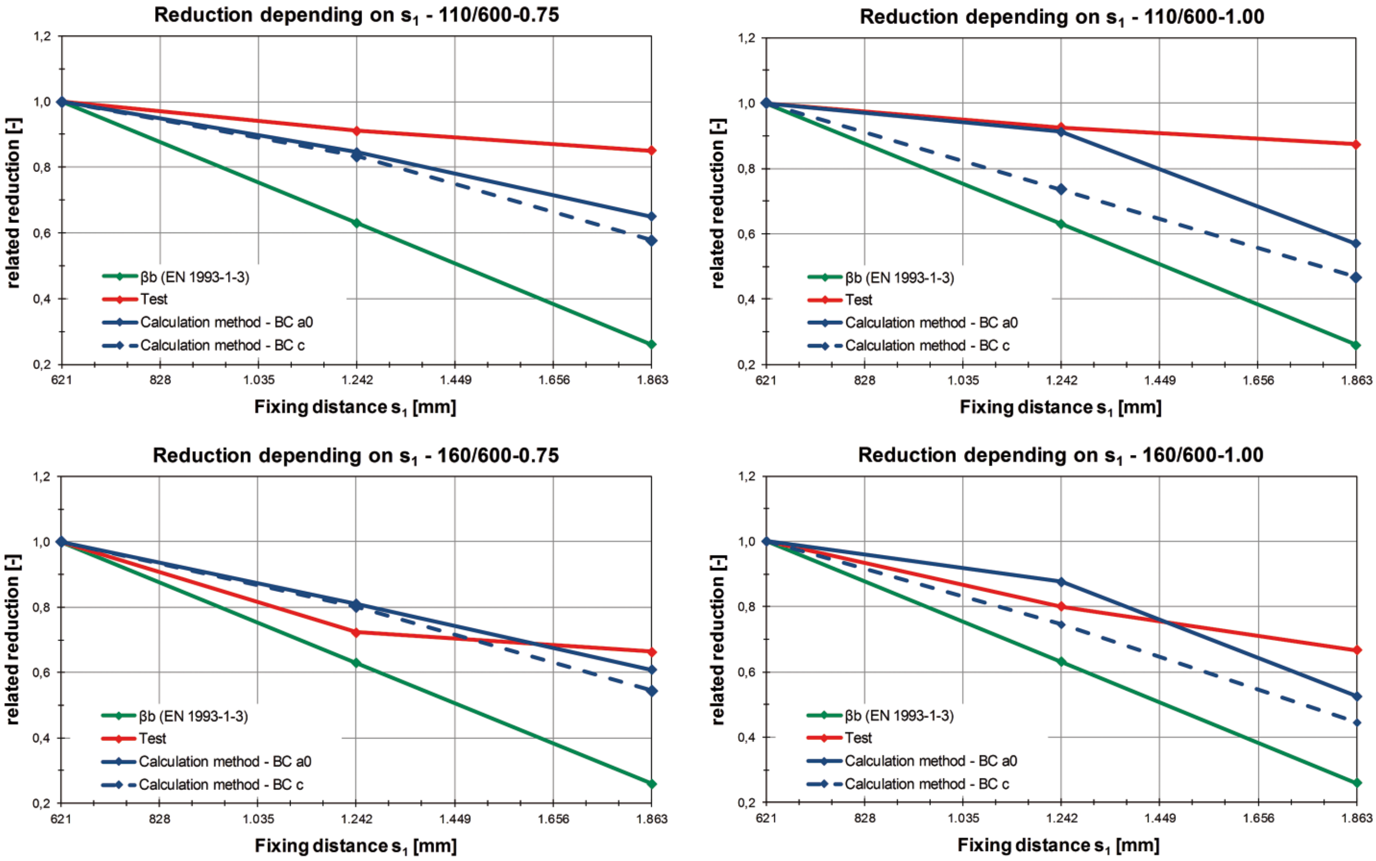

Fig. 9. Comparison of the calculation method with the test results and the reduction according to DIN EN 1993-1-3

step 3, the calculated values for liner tray 110/600 are between the test values and the values according to EN 1993-1-3. For liner tray 160/600, the values are partly above the test values and the load capacities are slightly overestimated, which can be explained, on the one hand, by the test scattering for liner tray 160/600-0.75 and, on the other, by the specific detection of the elastic bedding in step 3.

4 Conclusions

The first part of this paper compared different solutions for improving the thermal performance of liner tray wall systems. The results of the numerical investigations have shown that, from a building physics point of view, the option with an additional insulation layer is the best option for limiting the heat transfer between the outer shell and the liner tray. Some constructional disadvantages, such as the fact that the weight of the outer shell must either be suspended from the eaves or supported at the base, lead to a need for further research in this area. The option with spacer sections raises the question of the influence of the fixing distance s_1 on the mechanical performance of liner tray wall systems. Therefore, the second part dealt with the investigations that were carried out within the framework of the European RFCS research project GRISPE. Extensive experimental investigations on liner trays with a directly fixed outer façade were performed at KIT Steel and Lightweight Structures, and a new practicable design method has been derived based on existing regulations and methods.

Acknowledgements

The results and calculation methods presented in this paper were developed in studies carried out within the scope of the European RFCS research project GRISPE (RFCS-CT-2013-00018), co-financed by the “Research Fund for Coal and Steel” of the European Union, in which the Karlsruhe Institute of Technology (KIT) and the Engineering Office for Lightweight Construction were research partners. The design manual, software and eLearning materials for this method from the dissemination project GRISPE+ can be found free of charge on the website http://www.grispeplus.eu/. We would like to take this opportunity to express our thanks for the financial support. We would also like to thank the other research partners, L’enveloppe Métallique du Bâtiment (EMB), Bacacier Profilage SAS, Société Bretonne de Profilage SAS (Joris Ide) and Sokol Palisson Consultants SARL, for their excellent and constructive cooperation.

References

[1] EN 1090-4: Execution of steel structures and aluminium structures – Part 4: Technical requirements for cold-formed structural steel elements and cold-formed structures for roof, ceiling, floor and wall applications. Sept 2018.

[2] EN 1993-1-3: Eurocode 3: Design of steel structures – Part 1-3: General rules – Supplementary rules for cold-formed members and sheeting. Dec 2010.

[3] EN ISO 6946 – Building components and building elements – Thermal resistance and thermal transmittance – Calculation methods. Mar 2018.

[4] EN ISO 10211: Thermal bridges in building construction – Heat flows and surface temperatures – Detailed calculations. Mar 2018.

[5] Kuhnhenne, M.; Ungermann, D.; Brieden, M.; Wiegand, A.: Building redevelopment – Solutions for roof and façade using lightweight steel construction. *Stahlbau* **86** (2017), No. 10.

[6] Kuhnhenne, M.; Ungermann, D.; Brieden, M.; Wiegand, A.: New Solutions for energetic improvement of building envelopes in lightweight steel. *Stahlbau* **87** (2018), No. 11.

[7] EN ISO 10456: Building materials and products – Hygrothermal properties – Tabulated design values and procedures for determining declared and design thermal values. May 2010

[8] DIN 4108-4: Thermal insulation and energy economy in buildings – Part 4: Hygrothermal design values. Mar 2017.

[9] IFBS-Fachinformation 4.02: Bauphysik – Fugendichtheit im Stahlleichtbau, Düsseldorf, IFBS e.V., Nov 2004.

[10] Kuhnhenne, M. et. al.: Effective thermal insulation by application of steel cassette profiles. *Stahlbau* **82** (2013), No. 11.

[11] National Annex – Nationally determined parameters – Eurocode 3: Design of steel structures – Part 1-3: General rules – Supplementary rules for cold-formed members and sheeting. Dec 2010.

[12] DIN 18807-2: Trapezoidal sheeting in building; trapezoidal steel sheeting; determination of loadbearing capacity by testing, Jun 1986.

[13] DIN 18807-2/A1: Trapezoidal sheeting in building – Steel trapezoidal sheeting – Execution and evaluation of ultimate strenth tests; Amendment A1, May 2001.

[14] Misiek, T.; Käpplein, S.: Loadbearing behaviour of liner tray walls with directly or indirectly fixed outer façades. *Stahlbau* **84**, No. 11, pp. 875–889, Nov 2015, https://doi.org/10.1002/stab.201510328.

[15] EN 10346: Continuously hot-dip coated steel flat products for cold forming – Technical delivery conditions, Oct 2015.

[16] KIT Steel and Lightweight Structures.

Authors
Univ.-Prof. Dr.-Ing. Markus Kuhnhenne
mku@stb.rwth-aachen.de
Dipl.-Ing. Dominik Pyschny
dpy@stb.rwth-aachen.de
Lisa Kramer, MSc
lkr@stb.rwth-aachen.de
Dipl.-Ing. Matthias Brieden
m.brieden@stb.rwth-aachen.de

RWTH Aachen University,
Lehr- & Forschungsgebiet Nachhaltigkeit im Metallleichtbau
Mies-van-der-Rohe-Str. 1
52074 Aachen, Germany

Univ.-Prof. Dr.-Ing. Thomas Ummenhofer
thomas.ummenhofer@kit.edu
Dr.-Ing. Daniel C. Ruff
daniel.ruff@kit.edu
Dipl.-Ing. Christian Fauth
christian.fauth@kit.edu

KIT Stahl- & Leichtbau
Versuchsanstalt für Stahl, Holz & Steine
Karlsruher Institut für Technologie (KIT)
Otto-Ammann-Platz 1, 5 & 7
76131 Karlsruhe, Germany

Dipl.-Ing. Rainer Holz
Ingenieurbüro für Leichtbau
Rehbuckel 7
76228 Karlsruhe, Germany
rainer.holz@ifleichtbau.de